URTeC: 539

Compositional Tracking of a Huff-n-Puff Project in the Eagle Ford

M.L. Carlsen*[1], C.H. Whitson*[1,3], M.M. Dahouk[1], B. Younus[1], I. Yusra[1], E. Kerr[2], J. Nohavitza[2], M. Thuesen[2], J.H. Drozd[2], R. Ambrose[2], S. Mydland[3] 1. whitson, 2. EP Energy, 3. NTNU

This paper was prepared for presentation at the Unconventional Resources Technology Conference held in Denver, Colorado, USA, 22-24 July 2019.

Abstract

The objective of this paper is to help understand the mechanisms behind gas-based enhanced oil recovery (EOR) seen in actual field performance. This is accomplished by computing and interpreting daily wellstream compositions obtained from production data during the production period(s) of Huff-n-Puff (HnP) wells in the Eagle Ford, together with relevant PVT and numerical modeling studies.

Wellstream compositions are determined from readily available production data using an equation of state (EOS) model and measured oil and gas properties obtained from sampling at the wellhead. The wellstream composition is estimated daily in one of the following two ways: (1) if measured properties from field sampling are available, then regress to find a wellstream composition that matches all the measured oil and gas properties (e.g. stock-tank oil API, gas specific gravity, GOR, and separator fluid compositions). (2) if no measured properties from field sampling are available, then flash the most-recent wellstream composition estimated from (1) and recombine the resulting oil and gas streams to match the producing GOR.

Multiple lab-scale HnP EOR experiments and associated results have been published earlier, but only limited amounts of compositional data have been presented. In this study, we attempt to link produced wellstream compositions with simulated laboratory compositions reflecting different EOR recovery mechanisms. These results should enhance the understanding of the HnP EOR mechanisms to further optimize injection and production strategies, ultimately leading to higher recoveries. The data and observations from this analysis are presented in detail. The wellstream compositions before and after HnP implementation are shown and interpreted.

By providing daily estimates of oil and gas compositions, the compositional tracking technology presented in this paper can be used as a tool to understand key mechanisms behind the reported uplift seen in EOR in unconventional resources. The identification of these mechanisms is important for companies that are implementing EOR, because it allows them to optimize their EOR strategies, target higher recoveries, and increase the technical certainty in reserve booking.

Introduction

After EOG Resources reported uplift results from their Eagle Ford Huff-n-Puff (HnP) activities, gas injection has gained significant traction in tight unconventionals. The HnP method is fundamentally different from a conventional displacement process. While a traditional gas injection project relies on injection wells and production wells, the HnP scheme uses a single well that is both injecting (huff) and producing (puff) through the same wellbore, in a cyclic manner. The injection period is sometimes followed by a subsequent soaking (shut-in) period.

Several HnP-related, lab-scale EOR experiments and associated results have been published (Alharthy et al. 2015, Hawthorne et al. 2017, Liu et al. 2018, Tovar et al. 2018). A wide range of reservoir simulation studies have also been conducted on this topic (Atan et al. 2018, Hamdi et al. 2018, Sahni et al. 2018, Fiallos et al. 2019). Field performance results have been documented using public data coupled with comprehensive analytical model studies by Hoffman (2016, 2018, 2019).

In this study, we attempt to use a HnP field project in Eagle Ford as a large-scale PVT laboratory. This is done by analyzing produced wellstream compositions with time and comparing these to compositions reflecting different EOR recovery mechanisms. These results can enhance the understanding of the EOR mechanisms to further optimize injection and production strategies, ultimately leading to higher recoveries.

To make it possible for others to reproduce the PVT and reservoir simulation *modeling* results presented in this paper, the EOS and associated compositions are provided in **Table 1** and **Table 2**. However, this EOS is "generic" and not the same as the one used specifically for the compositional tracking of the Eagle Ford HnP project (which is confidential).

Gas EOR Fundamentals

Miscibility. In petroleum engineering, we consider two types of miscibility: *first-contact miscibility (FCM)* and *multi-contact miscibility (MCM)*.

First-Contact Miscibility. At a given pressure and temperature, first-contact (FC) miscibility refers to the process in which two fluids mix in all proportions – at any concentration of either fluid – such that the resulting mixture remains a single phase. This is the formal, text-book definition of "miscibility".

In petroleum systems, we use the term *first-contact miscibility pressure* (FCMP) to define any pressure at which the injection gas and reservoir fluid mix on first contact (in any proportion), forming a single phase. The *minimum first-contact miscibility pressure* (MMP_{FC}) is obtained from a swell test, defined as the maximum pressure on a p-x diagram (saturation pressure vs. mol% injection gas); shown in **Fig. 1**, for a *rich* and a *lean* injection gas.

Above the MMP_{FC}, the reservoir fluid is *always* single-phase (oil or gas) after the injected gas has contacted the oil. Below the MMP_{FC}, the reservoir fluid *may* be single-phase (oil or gas) but it will be two-phase for some mixtures of injected gas and reservoir fluid.

Multi-Contact Miscibility. In a conventional displacement process, miscibility between a reservoir fluid and an injection gas develops through a dynamic process of mixing, with component exchange controlled by phase equilibria (K-values) and local compositional variation along the path of displacement. In such a process, the injection gas and reservoir fluid are said to be multi-contact miscible (MCM). Multi-contact (dynamic) miscibility investigates the mixtures that form as a result of interaction of phases with different compositions flowing at different velocities in a porous medium (Jessen & Orr, 2008).

Minimum Miscibility Pressure. For a given temperature, injection gas composition, and reservoir fluid composition, the *minimum miscibility pressure* (MMP) is the lowest pressure at which first- or multi-contact miscibility can be achieved for a specific process, e.g. MMP_{FC}, MMP_{VGD}, and $MMP_{C/V}$.

Vaporizing Gas Drive & Condensing Gas Drive. Before 1986, it was believed that developed/multi-contact miscibility followed one of two paths: (1) vaporizing gas drive (VGD), developed and maintained at the gas front; or (2) condensing gas drive (CGD), initiated at the point of injection behind the gas front. In a VGD process, the injection gas becomes enriched in C_{2+} by multiple contacts with the original reservoir fluid, and miscibility is eventually developed at the *gas front*. In a CGD process, the injection gas containing light intermediates (e.g. C_2-C_5) was *mistakenly* assumed to continuously enrich the reservoir oil at the *point of injection* until the injection gas and the enriched reservoir oil become miscible (Zick, 1986, Stalkup, 1984).

Combined Condensing/Vaporizing Mechanism. In 1986, Zick was the first to show that a combined vaporizing and condensing (C/V) mechanism describes the actual development of minimum miscibility for *most* naturally occurring petroleum systems. He showed that the point of miscibility, i.e. ~100% recovery efficiency in a dispersion-free 1D displacement, is somewhere *between* the point of injection and the gas front, as shown in **Fig. 2**.

Zick (1986) also found that the MMP predicted by the C/V mechanism could be significantly lower than the one predicted by the VGD mechanism; findings that have later been verified by many since then (Orr et al., 1991; Johns et al., 1992; Hearn & Whitson, 1995).

Zick (1986) also explained why the CGD mechanism will seldom (if ever) develop in petroleum systems[1]. This is because after a few contacts with fresh injection gas, the oil becomes saturated in light intermediates (e.g. C_2-C_4) but continues to lose middle intermediates and light heavies (C_{5+})[2] that are stripped out and carried away (*vaporized*) by the more mobile gas phase that does not contain these heavier components. Put simply; what starts out as *net condensation* of light intermediates, making the oil lighter, turns into a never-ending, *net vaporization* of C_{5+} from the oil. Once this happens, the oil continuously gets heavier and has no chance of becoming miscible with the gas.

True MMP. The "theoretical" *true* minimum miscibility pressure is formally the pressure resulting in 100% oil recovery during a dispersion-free, 1D displacement process after 1 pore volume injected (PVI). Experimentally, a properly-conducted slimtube test yields the true MMP (albeit slightly higher than thermodynamic MMP, because of small physical dispersion resulting in slightly less than 100% recovery at 1 PVI).

A characteristic for practically all petroleum systems, is that the MMP_{FC} is higher than the multi-contact MMPs ($MMP_{C/V}$ and MMP_{VGD}). If the C/V mechanism develops then its $MMP_{C/V}$ is the true MMP and will be lower than the MMP_{VGD}. For very lean injection gases (e.g. N_2 or C_1) the C/V mechanism may not develop, in which case the true MMP is by the VGD mechanism. As an example, the compositions given in Table 1 yield the following MMP predictions at T = 250 F:

(a) reservoir oil and *rich* injection gas: MMP_{FC} = 5560 psia. MMP_{VGD} = 5336 psia. $MMP_{C/V}$ = 4157 psia

(b) reservoir oil and *lean* injection gas: MMP_{FC} = 8686 psia. MMP_{VGD} = 6442 psia. $MMP_{C/V}$ = 6426 psia.

The $MMP_{C/V}$ can be computed by a multi-cell calculation process such as a 1D slimtube simulation, with proper treatment of numerical dispersion (Stalkup, 1990; Hearn & Whitson, 1995). The MMP_{FC} and MMP_{VGD} can be computed from a simple, single-cell, multi-contact PVT simulation – FC by a swelling test and VGD by a forward-contact PVT test. Most commercial PVT software packages do not provide the accurate determination of $MMP_{C/V}$; this is unfortunate, given that $MMP_{C/V}$ is usually the true MMP.

[1] Real petroleum systems refer to petroleum systems found in nature (not ternary systems), with 1000s of petroleum compounds

[2] Middle intermediates: Components present in the oil but not significantly present in the injection gas. These are the components that can be vaporized by the oil. The lightest components in this group typically ranges C_4-C_{10}, depending on injection gas composition, while the heaviest is somewhere around C_{30}

Gas Huff-n-Puff – Fundamental Phase Behavior

Huff-n-Puff Characteristics. Because the HnP process is not a displacement process, the key mechanisms behind developed miscibility found in the conventional gas injection literature (e.g. $MMP_{C/V}$) are less relevant. During the 30-90 day injection periods typically seen in HnP field projects, the main objective is not to displace the oil from a producer to an injector, but rather for the gas to contact and mix with as much oil as possible: dissolving/vaporizing oil components into the gas or mix with and swell the oil.

Gas EOR Experiments Performed on Shale/Tight Core Plugs. Hawthorne et al. (2017) performed gas EOR experiments on small core plugs (1.1 cm diameter x 4 cm long) in which the cores were submerged in a static bath of injection gas. The soaking was performed for 24 hours at a constant temperature and pressure, and oil recovery was reported over time for a range of different injection gas compositions as shown in **Fig. 3**. In these experiments, the size of the core plugs was small enough and the short soak time sufficiently long for the gas to diffuse/disperse into the rock and mix with the oil.

Because the injection gas mixes substantially with the oil, these experiments become directly relatable to what is expected when injecting gas into a PVT cell, at which instantaneous mixing phase equilibrium is achieved. To exemplify this, the different injection gases can be repeatedly introduced into a PVT cell, initially filled with oil[3], at a constant pressure, volume, and temperature. The simulations of such an experiment is presented in **Fig. 4**, and as seen, they are consistent with the rock/fluid results documented by Hawthorne et al. (2017) and others (Jin et al. 2017). Note how very similar behavior can be observed in the *rock/fluid experiments* presented in Fig. 3**,** and the *pure PVT experiments*[4] presented in **Fig. 4**:

1. The recovery efficiencies are fundamentally different at p_{inj} above and below the MMP_{FC}
2. $p_{inj} > MMP_{FC}$: the primary recovery mechanism is *pure mixing/swelling*
3. $p_{inj} < MMP_{FC}$: the primary recovery mechanism is a combination of *pure mixing/swelling* (when single-phase) and *vaporization* (when two-phase)
4. Lower MMP_{FC} yields higher recovery efficiency, and higher MMP_{FC} yields lower recovery efficiency

HnP PVT Experiment. In contrast to the constant pressure experiments conducted by Hawthorne et al. (2016), the HnP process is characterized by

1) an *injection period* with associated pressure *build up* until some maximum pressure (p_{max}) is reached, typically determined by local fracture gradients and/or confinement
2) *a production period* with associated pressure *depletion* until some minimum pressure (p_{min}) is reached

The PVT experiments that are typically run in tandem with gas EOR screening studies (multi-contact, slimtube, rising bubble apparatus, vanishing interfacial tension) are designed for conventional displacement processes and do not really serve the purpose of capturing relevant phase behavior for HnP EOR in tight unconventionals. We recommend a more relevant PVT experiment that incorporates the characteristics of the HnP process. This is achieved by creating a hybrid of the swelling test and a constant volume depletion (CVD) experiment. The new proposed experiment consists of the following steps:

[3] Here the oil composition presented in Table 1 is used.

[4] We emphasize that this is not an attempt to reproduce the results by Hawthorne (Hawthorne et al. 2017), as the oil composition and the amount of gas injected from those experiments was not available during this analysis. Neither was the same reservoir temperature used, or the EOS tuned to the relevant PVT data.

1. First, a constant volume injection (CVI) experiment is performed, in which gas is injected into the PVT cell at a constant volume until a maximum pressure p_{max} is reached. This is basically an *isovolume* swelling experiment and it is mimicking the injection (huff) period.
2. This is followed by a constant volume depletion (CVD) experiment, in which fluid[5] is removed from the PVT cell while keeping the volume constant until a minimum pressure p_{min} is reached. This is mimicking the production (puff) period. Considering lab practicalities, we suggest to only do a single-stage CVD to save both time and cost. An important distinction from a traditional CVD experiment is that the initial volume in the PVT cell can be 2-phase, while a conventional CVD experiment starts at the saturation pressure, i.e. at which the cell volume is single phase.
3. Step 1) and 2) are then repeated several times (HnP cycles).

Fig. 5 shows a conceptual illustration of the experimental design. This PVT experiment has all the key characteristics of the HnP process: i) *injection periods* with associated pressure build-up, ii) *production periods* with associated pressure drawdown, iii) a *cyclic* nature, and iv) *oil recovery* versus number of cycles and/or relative moles (volume) of gas injected.

Fig. 6 shows an example of the oil recovery factor[6] from a HnP PVT experiment with pressure cycling between p_{min} = 1000 and p_{max} = 6000 psia (Δp = 5000 psia) for 10 cycles with different injection gases. **Fig. 7** shows the same example for a *higher* pressure cycling interval between p_{min} = 1000 and p_{max} = 10000 psia (Δp = 9000 psia). Note how a higher p_{max} increases the recovery factor, but this is simply because more moles of gas are injected into the PVT cell and vaporize more of the oil components. The recovery efficiency[7] (recovery per mole injected), however, does not change, as seen by comparing the *recovery factor* (RF) versus *relative moles injected* (RMI) shown in **Fig. 8**.

In such a cyclic process, the MMP_{FC} is an important parameter, because the recovery characteristics observed above and below this pressure are fundamentally different.

Mixing. Imagine you have a cup half filled with *saltwater*. You fill up this cup by adding half a cup of *freshwater*. Then you stir and remove half of the mixed fluid. Now you will have half of the original salt concentration. If you repeat this, you will eventually end up with only freshwater in the cup. This process is a *pure mixing* – or *dilution* – process at which the fluid composition in the cup, originally saltwater, converges to the composition of the injectant, here freshwater. This saltwater dilution process is analogous to what happens in the HnP PVT experiment if pressure cycling occurs above the MMP_{FC} ($p_{min} > MMP_{FC}$), in which the cup is the PVT cell, the saltwater is the original reservoir fluid, and the freshwater is the injectant. Above the MMP_{FC} the fluid in the PVT cell is *always* single-phase, i.e. a *pure mixing process*, and the volume is removed from the cell due to volume-increase (swelling).

Vaporization. In the HnP PVT experiment, when pressure cycling occurs below the MMP_{FC} pressure ($p_{min} < MMP_{FC}$), the PVT cell *may* be occupied by a single-phase fluid in a few of the early cycles, but eventually the PVT cell volume will become two-phase. The oil recovery will then be a result of vaporization in which the intermediate components from the oil vaporize into the injection gas during each injection (huff) period and are produced/ "stripped out" during each production (puff) period.

[5] At pressures above the MMP_{FC}, the PVT cell is occupied with single-phase oil or gas.
[6] The C_{6+} of the original reservoir fluid is used as a measure of oil recovery as the enhanced recovery target is mainly represented by the C_{6+} of the original reservoir fluid.
[7] Enhanced oil recovery (EOR) efficiency is additional oil recovered per volume of gas injected; in this case RF_{C6+} /relative moles injected. In the field it is typically expressed in units of STB/MMscf.

Comparison of Different Mechanisms. To understand the fundamentals behind the observed uplift, three scenarios were analyzed in which the lowest cycling pressure (p_{min}) is

a. below the bubblepoint pressure of the reservoir oil ($p_{min} < p_{sat} < MMP_{FC}$)

b. above the bubblepoint pressure, but below the MMP_{FC} of the reservoir oil ($p_{sat} < p_{min} < MMP_{FC}$)

c. above the MMP_{FC} of the reservoir oil ($p_{sat} < MMP_{FC} < p_{min}$)

All scenarios are analyzed at T = 250 F, with the reservoir oil and *rich* injection gas presented in **Table 1**. **Fig. 9** shows the oil recovery versus relative moles injected for the three scenarios mentioned above. Note how the p_{min} relative to the MMP_{FC} yield three fundamentally different results.

Scenario a ($p_{min} < p_{sat} < MMP_{FC}$) shows a process dominated by vaporization only, with relatively low "recovery efficiency" (slope). This process is characterized by fresh injection gas contacting and equilibrating with the oil, stripping out small amounts of intermediates, and light "heavies", from the oil in each cycle.

Scenario b ($p_{sat} < p_{min} < MMP_{FC}$) is especially interesting because it changes slope after a few contacts. First, it is a process dominated by pure mixing (saltwater analogy). Thereafter, the main recovery process changes and is dominated by vaporization only, which has a lower recovery efficiency (slope). This happens because the gas and oil mix into a single phase the first few cycles, even though they are not fully miscible (do not mix in *all* proportions). The change of the slope coincides with the saturation pressure (initially 2500 psia) of the altered fluid composition (after a few contacts) becoming higher than p_{min}, i.e. 4000 psia.

Scenario c ($p_{sat} < MMP_{FC} < p_{min}$) shows a process dominated by mixing only (saltwater analogy), because p_{min} is above the MMP_{FC} for all cycles[8]. Note how the recovery efficiency of the pure mixing mechanism is the most efficient.

Characteristics of HnP Produced Wellstreams – PVT experiment. If the PVT lab and budget allow for it, a recommended modification of the PVT HnP experiment proposed above is to perform a multi-stage, instead of a single-stage, CVD experiment during the production (puff) period as illustrated in **Fig. 10** and **Fig. 11**. This is more representative of the actual production (puff) period, at which hydrocarbons are produced at different, decreasing pressures in each cycle. More stages will result in a higher oil recovery, as seen in **Fig. 12**, because some of the production occurs at pressures in which the EOR efficiency is higher – e.g. above the p_{sat}.

By analyzing the compositions of the recovered fluid at each stage, in each cycle, as illustrated in **Fig. 13**, the following observations can be made

- Stock tank liquid API, γ_{API}: At constant APIs, the recovery efficiency is high. If the API increases as pressure decreases, this coincides with a lower recovery efficiency.
- GOR: At constant GORs, the recovery efficiency is high. If the GOR increases when pressure decreases, this coincides with a lower recovery efficiency.
- Produced wellstreams, z_i: the compositions removed will eventually converge to the composition of the injection gas. Eventually, all the surface oil (C_{6+}) is recovered.

If you observe <u>constant</u> producing GOR (R_p), API, and produced wellstream compositions for some fraction of the HnP production period, then you should expect a high EOR efficiency. A lower EOR efficiency coincides with increasing GORs and APIs.

[8] The MMP_{FC} changes slightly after each contact, but the change is negligible. In this case, the MMP_{FC} changes from 5560 psia (initial reservoir oil) and decreases to 5517 psia after the 10^{th} cycle.

Gas Huff-n-Puff – Compositional Reservoir Simulation

Reservoir Simulation Pitfalls when Modeling the HnP Process. The HnP PVT experiment proposed above is an idealized process and does not consider aspects such as time, spatial pressure variations, non-ideal mixing, diffusion/dispersion, confinement/containment issues, fluid heterogeneity, and fracture/matrix flow. Hence, the experimental data from such a PVT test should first and foremost be used to tune an EOS model that will then be used in a (compositional) reservoir simulator. However, there are several pitfalls that should be avoided when modeling the gas HnP process, even with a 'perfect' EOS model.

Numerical dispersion. First, a proper grid sensitivity study should be performed. In compositionally sensitive processes such as gas EOR, insufficient gridding can result in significant *numerical dispersion* (Coats, 2005). This can lead to an artificially *low* recovery in a miscible gas displacement process (conventionals). Ironically, numerical dispersion in modeling of a HnP process (unconventionals) will lead to an artificially *high* recovery. Adequate grid resolution for a HnP model, i.e. without numerical dispersion, might be several orders of magnitude greater than what is necessary to model primary depletion. Numerical dispersion that mimics *physical dispersion* in a displacement process can be incorporated using the methods proposed by Lantz (Lantz, 1971, Cheng, 2005).

Shattered rock volume. If a dual porosity (DP) region is used in the model, it should, in its most rigorous implementation, match single-porosity (SP) behavior to ensure physically consistent results (Coats, 1989). **Fig. 14** shows the performance of a DP model that mimics the performance of a (numerically converged) SP model during *primary depletion.*

In unconventionals, the dual porosity (DP) region represents a region of "*shattered rock volume*" (SRV). **Fig. 15** shows how the HnP performance of the DP model and SP model differs[9]. The DP model represents a region at which the rock pieces are small enough for the gas to diffuse and disperse into the rock, mixing with much of the reservoir fluid found in the SRV rubble during each HnP cycle. In these simulation results, the pure mixing/swelling can be substantial, and significant uplift is observed. The SP model, on the other hand, is simply a "slab of rock" that will essentially yield no additional HnP recovery. Injection and production, in and out of the rock outside the SRV, will result in a piston-like displacement with neglible incremental recovery - a Sisyphean process. This is consistent with the observations made by Kanfar & Clarkson (2017) when studying the SP model; "*incremental recovery, and hence the success of huff-n-puff, is artificially improved due to coarse gridding. Conversely, with finer gridding, recovery is not improved, or is lower than for primary recovery".*

Characteristics of HnP Produced Wellstreams – Reservoir Simulation. The produced wellstream compositions of (1) a SP model with *no* SRV, and (2) a DP(SRV)/SP model are presented in **Fig. 14** and **Fig. 15** – the two models showing strongly differing production *signatures* for a HnP process. **Fig. 16** compares the API, GOR and wellstream compositions for the SP model without SRV, showing *no incremental uplift*, and an "equivalent*"* dual porosity DP model showing *substantial incremental uplift*. Important observations include:

- *Single porosity (SP) model - no incremental uplift*: high GORs, high APIs and high wellstream C_1 content are observed *early* in each production period, with precipitous changes after flowback of the injected gas. The opposite trend is seen for C_{7+} in the wellstream because the injected gas creates a piston-like displacement into the reservoir, flowing back the injected gas (no C_{7+} content) before oil volumes being produced prior to gas injection resume production (high C_{7+} content).

[9] Injection and production cycles are 30 days, respectively. Injection pressure is p_{inj} = 8000 psia, while production pressure is p_{wf} = 1000 psia.

- *Dual porosity (DP) model - substantial incremental uplift:* GOR and methane content increase within each production period, and, from one HnP cycle to another. Liquid APIs increase within each HnP cycle but span a wider range of APIs as the number of cycles increase. The C_{7+} content decreases substantially from one HnP cycle to the next. Note how these trends are very similar to the compositional trends seen in the HnP PVT experiment shown in Fig. 13.

Recommendation for Modeling Huff-n-Puff. The premise for uplift in a gas HnP process is the existence of a shattered rock volume (SRV) with small enough pieces of *rubble* (pieces of rock that are small in one dimension), leading to substantial mixing of the injection gas and reservoir fluid found during the injection/soak period (~1-3 months).

There are two key elements of the SRV region: (i) the size of the SRV (= target oil EOR), and (ii) the distribution of the rubble's minimum dimension, L_{min}. Both properties are key uncertainties and should be treated as history matching parameters. Distribution bounds can be estimated using 1) simplified RTA methods (Acuña, 2018), 2) tracers (~$q_f(t)$ w/mass balance), 3) geomechanical modeling, 4) DFITs, 5) flowback data, 6) micro-seismic, 7) coring (Raterman et al., 2017), 8) geological interpretation and 9) formation imaging. To ensure consistency in the modeling of a HnP recovery process, from core to field scale, the following workflow is recommended:

1. **Rubble-Fracture Single-Porosity Modeling**: Model a range of single pieces of rubble (e.g. 2, 10, 30 and 100 cm) surrounded by a "fracture", with cycle times of ~30 days, in which all "physics" are included. Use a tuned equation of state (EOS) model and a compositional reservoir simulator, with gridding that minimizes numerical dispersion, but mimics physical dispersion (Coats et al., 2004). Include diffusion, where diffusion coefficients have been fit to laboratory experiments with relevant rock and fluid. Model the experimental recovery for 30 days for the different "rubble sizes". The end-cycle recovery is expected to be inversely proportional to the rubble size.
2. **Upscaling:** Modeling every single size of rubble on a field- or well-scale is impractical, if not impossible. Hence, to scale up the rubble-fracture modeling results, we suggest creating a *dual porosity* model with transfer term(s)[10] between matrix and fracture, T_{mf}, being set to values that replicate the recovery responses seen in the rubble-fracture SP modeling. The DP model is only used to model the SRV.
3. **Field/Well-Scale Modeling:** The well model will include, i) a dual-porosity region (representing the *shattered rock volume*), and ii) a single-porosity region (tight rock with no fractures). This model must be history matched to production data, while honoring the pseudo model based on the core scale modeling. As mentioned earlier, the key history-matching parameters (for EOR purposes) are SRV size, and rubble size distribution.

Gas Huff-n-Puff – Field Project in the Eagle Ford

The project studied in this paper is a multi-well project in which one of the wells in the lease is subject to cyclic HnP gas injection, while the other wells remained producers. Despite gas injection taking place only in one of the wells, injected gas was clearly reaching the offset wells (well spacing approx. 500 ft). To mitigate gas cycling and allow for the pressure in the lease to build up, the offset wells were shut in during the injection period. The effect of injected gas reaching offset wells was not only seen during the injection period with pressure build up, but also, during the production period at which increased production was observed (when compared to DCA forecasted rates). The first HnP cycle started in early 2018. Each of the injection and production periods had a duration of 2-3 months.

[10] Some simulators, such as Sensor from Coats Engineering, use two matrix-fracture transfer terms, one for Darcy-driven flow and the other for diffusion-driven flow.

Most of the data made available for this project are treated as confidential, including production and fluid sampling data, and therefore cannot be presented in this paper. The production data used includes daily separator rates for oil, gas, and water (separator oil density obtained from Coriolis meters), at separator pressure and temperature. The fluid sampling data includes a few points with analysis of the separator gas composition (up to C_{7+}) and liquid API. The data received includes the production profile resulting from two HnP cycles.

Compositional Tracking. In this paper, *compositional tracking* refers to monitoring the produced wellstream compositions (z_i), separator compositions (x_i & y_i), and stock tank liquid API over time. This can be achieved in two ways. Either separator samples are collected, sent to the lab and *physically* recombined to a wellstream composition every single day with associated analysis. However, this is expensive, time-consuming, and impractical. The other option is to use an EOS model, together with readily available production and sampling data, to *compute* daily wellstream compositions. This method is leveraged in this study.

Methodology. A basin-wide EOS model tuned to a large set of PVT experiments covering the whole spectrum of fluids produced in the Eagle Ford (GORs from 300 to 200,000 scf/sep.bbl)[11] has been used. The wellstream composition is estimated in either of the following ways, for a given day, depending on the data available for that day:

1. **Fluid Sampling Data is Available (Whitson & Sunjerga, 2012):** regress to find a wellstream composition that matches all the measured oil and gas properties, e.g. stock-tank oil API, gas specific gravity, GOR, and separator fluid compositions. The regression is performed by adjusting: (i) the molar gas fraction of the wellstream, f_g, (ii) the wellstream composition of lighter components (C_1-C_6, H_2S, CO_2 and N_2) and (iii) the average molecular weight of heavier components, i.e. the C_{7+} fraction. The EOS model component properties and binary interaction parameters (BIPs) remain unchanged through this regression.
2. **Only Production Data is Available (Hoda & Whitson, 2013):** flash the most-recent wellstream ("feed stream") composition estimated from (1) and recombine the resulting oil and gas streams to match the producing GOR.

This will result in wellstream compositions that honor all daily measured production data.

Characteristics of HnP Produced Wellstreams – Field Observations. The production and fluid sampling data were successfully used to predict daily wellstream compositions for the well subject to cyclic gas injection.

Separator oil densities were not used as part of the wellstream composition prediction algorithm but were used to validate the accuracy of the method. This was done by first flashing the predicted wellstream compositions to the separator conditions associated with the Coriolis meter readings. Then, the predicted separator oil composition was used to predict the liquid density.

The comparison of predicted vs measured separator oil densities is shown in **Fig. 17**. The "X" symbol marks the points in time for which additional fluid sampling data is available. Generally, the prediction falls within the ±2% from the measured densities. However, one important observation is that the prediction is improved with the sampling data availability, i.e. "poorer" density predictions coincide with less frequent sampling data. For instance, many sampling points are available during the *first* HnP cycle (*very* good predictions), while no sampling points are available during the *second* HnP production cycle (*less* good predictions). Therefore, to ensure a correct implementation of the compositional tracking method, it is important to have enough fluid sampling data. Our recommendation is to sample properties

[11] This EOS model is not presented in this paper due to confidentiality. The model is a Peng-Robinson cubic EOS model, with 35 components (SCN from C6 to C30p).

(compositions and densities) of separator gas, separator oil, and stock-tank oil simultaneously to honor the material balance required for recombination.

Fig. 18 shows the predicted wellstream composition vs time for the HnP well. During depletion, the wellstream composition becomes leaner because the bottomhole pressure declines below the saturation (bubblepoint) pressure (p_b ~ 2500 psia), after around 20 days of production. The saturation pressure versus time is calculated using the predicted wellstream compositions and is shown in **Fig. 19**.

During the production periods, the increased GOR is reflected in the wellstream composition with an increased methane (C_1) content with respect to the depletion period. One observation from these figures is that the produced gas right after injection is not just the flowback of the injected gas (which contains less than 0.5% C_{7+}), but it is a mix of the injected gas with the reservoir oil, resulting in a wellstream C_{7+} content of 2-10%. Another important observation is that even by the end of the two HnP cycles, the wellstream composition is still leaner (higher C_1 content) than the wellstream composition seen during depletion, meaning that the well is still producing the resulting mix of injected gas and reservoir oil.

Fig. 21 shows the detailed compositional tracking results for the HnP with focus on the timeframe around the two HnP cycles. The computed GOR, liquid API, and wellstream C_1 and C_{7+} are presented. The first HnP cycle shows a comparable behavior to what is observed in the HnP PVT experiment and the HnP in in which a constant GOR and API are seen at the beginning of the production period, indicating a high recovery efficiency. This behavior is not observed in the offset wells during the first cycle, but for the second cycle, which could indicate that during the first cycle the pressure build up and associated mixing was not sufficient to achieve a high recovery efficiency in the offset wells.

Discussion

Compositional Tracking. In an ideal HnP project, one would sample the wellstream frequently with separator samples, send those samples to a PVT laboratory, and make all the measured properties available for history matching. The cost of obtaining such data on a frequent basis is prohibitive. However, sampling surface product volumes and properties (API / separator-oil densities, gas gravities) is feasible and less costly.

We show that standard well test data gives, indirectly, all wellstream characteristics discussed above using the wellstream estimation method presented in this paper. The key to the success of this method is accurate and frequent surface test data, together with an EOS model that predicts accurately the fluid behavior for a wide range of producing wellstreams (from original reservoir fluids to injection gas alone). Periodic compositional analysis of produced stock-tank oil during HnP production periods adds uniqueness and accuracy to the method.

Compositional Signature of the HnP Process. This paper tries to study the complexity of produced compositional wellstreams for a HnP process. The information contained in a wellstream composition, when combined with a valid EOS model, includes (a) producing GOR, (b) surface product properties that include oil density (API), gas gravity and product compositions, (c) individual-component amounts produced, and (d) saturation pressure of the wellstream composition. These wellstream properties, and their transients during production periods, give a clear “signature” of the HnP performance. This paper touches upon three different but related approaches to understand the characteristics of HnP produced wellstreams.

We show from modeling results that the produced wellstreams compositional and property variations during a HnP process are significant and characteristic, thereby making such information critical to the history matching and understanding of a HnP process.

PVT Experiment. The proposed HnP PVT experiment is meant to provide insights into the ongoing phase behavior during HnP, by assuming that perfect mixing (thermodynamic equilibrium) occurs during the injection period. For a single piece of sufficiently small rubble, this is a valid assumption, and it is therefore possible to track and use the fluid responses (i.e. API, GOR, and wellstream composition) to understand which EOR mechanism dominates the recovery.

Reservoir Simulation. An implied assumption from using a CVD process to mimic the production (puff) period in the proposed HnP PVT experiment, is that the oil has zero relative permeability. This is most likely not the case, and we therefore show how the fluid responses act when relative permeability and matrix/fracture flow is considered. We show that there is a significantly different characteristic between a 'piston like' HnP process (*single porosity = no incremental uplift*), and recovery obtained from cyclic gas injection in a "shattered rock volume" (*dual porosity = significant incremental uplift)*.

Field Data. To verify that experiment and reservoir modeling results are representative for the true behavior of gas HnP, actual field data of the fluid responses from a multi-well project in the Eagle Ford is presented. We show in this paper that it is crucial to extract information from the wellstream during the HnP cycles to better understand the recovery efficiency. Our intention is to continually analyze new data with the compositional tracking technology as more cycles become available. Two cycles were analyzed in this study.

Confinement. In any HnP project it is necessary to define a "control volume" that confines (albeit arbitrarily) the HnP well and its "neighbors". Within this HnP control volume we know accurately the produced rates and produced cumulative volumes during the puff periods. We also know how much gas has been injected during the huff periods. The main and critical unknown is how much of the injection gas "leaves" the HnP control volume, being "lost" and not-to-be produced during subsequent puff periods. This injected gas volume loss issue is typically referred to as "confinement" (i.e. lack of confinement).

For perfect confinement without loss of injection gas, and no interaction of the injection gas with reservoir fluids, the HnP process would behave essentially as "gas storage", though in a very-low-permeability system.

Hammock plot. The Eagle Ford HnP project discussed in this paper has observed a characteristic behavior in what we term the "hammock" plot shown in **Fig. 20**. This plot shows (for each HnP cycle) surface tubing pressure on the x-axis and "net cycle cumulative injected volume" on the y-axis. The y-axis represents the actual cumulative injected gas volume during the injection period (moving left to right); while during the production period the curve moves from right to left and represents the remaining unproduced (injection) gas volume. This plot is used to illustrate the pressure build-up during the injection period (huff) and how the pressure decreases as the well is put back on production (puff). Significant *hysteresis* is observed. In addition, an improved pressure buildup "efficiency" is observed in the second cycle where pressure builds more for a given volume injected than in the initial cycle.

Future Work. In the future, studies to understand and replicate injection/production responses with model features such as adsorption, gas hysteresis, and leak/off communication can be incorporated. This might be important when cycle-to-cycle variability exists, which is apparent in the hammock plot seen in **Fig. 20**. With proper phase behavior understanding and subsequent abilities to replicate field results, the economic certainty is enhanced when evaluating project implementations. The ultimate goal is to use this understanding for field delineation and improve the technical reserves certainty for booking and valuations.

Conclusions and Observations

This paper studies the gas HnP process from three different perspectives: (i) fundamental phase behavior, (ii) compositional reservoir simulation, and (iii) field-scale performance monitoring. To summarize:

1. The premise for uplift in a HnP process is a shattered rock volume (SRV) containing rubble (small pieces of rock) that experience substantial mixing of the injection gas and reservoir fluid during a typical injection/soaking period (~1-3 months).
2. The recovery efficiency from the SRV is related directly with
    a. Size distribution of the rubble, with smaller pieces having a higher efficiency.
    b. The difference between "*the pressure within the rubble"* and *"the saturation pressure of the fluid mixture within the rubble"*, at the end of each injection/soaking cycle. The greater this pressure difference, the higher the efficiency.
3. Multi-contact miscibility/MMP is *not* relevant to a gas HnP process.
4. Hawthorne et al. (2017) present high oil recoveries in gas HnP experiments conducted on small core plugs in a cyclic injection-production process at constant pressure. The recovery characteristic is very similar to that of a simple cyclic gas injection process within a PVT cell. This suggests that the core plugs are small enough and time is sufficient for the gas to diffuse and disperse into the rock and mix substantially with the oil during the test.
5. We propose a new HnP PVT experiment that captures the key characteristics of a HnP process: i) *injection periods* with associated pressure build-up, ii) *production periods* with associated pressure drawdown, iii) a *cyclic* nature and iv) *recovery* versus number of cycles and amount of injected gas.
6. Reservoir simulation of a field HnP process requires a multi-stage modeling procedure that incorporates small-scale rubble-fracture phenomena that must be upscaled to well models.
7. The key to the success of the compositional tracking method is accurate and frequent surface test data, together with an EOS model that predicts accurately the fluid behavior for a wide range of producing wellstreams (from original reservoir fluids to injection gas alone). Periodic compositional analysis of produced stock-tank oil during HnP production periods adds uniqueness and accuracy to the method.
8. Information derived from compositional tracking of a HnP field project yields a wellstream "signature" that improves our understanding of recovery efficiency and uplift. This should give a more reliable technical basis for booking reserves and optimizing the HnP process.

Nomenclature

API	= stock tank liquid API
f_g	= molar gas fraction = $(z_i-x_i)/(y_i-x_i)$, fraction
FCMP	= first contact miscibility pressure, psia
GOR	= gas-oil ratio, scf/STB
L_{min}	= minimum dimension of rubble-size, ft
MMP	= minimum miscibility pressure, psia
MMP_{FC}	= first-contact minimum miscibility pressure, psia
MMP_{VGD}	= minimum miscibility pressure by the vaporizing gas drive mechanism, psia

$MMP_{C/V}$ = minimum miscibility pressure by the combined condensing/vaporizing mechanism, psia

OOIP = original oil in place, STB

p_b = bubblepoint pressure, psia

p_{inj} = injection pressure, psia

p_{max} = maximum pressure | maximum cycling pressure, psia

p_{min} = minimum pressure | minimum cycling pressure, psia

p_{sat} = saturation pressure, psia

p_{wf} = flowing bottomhole pressure, psia

PVI = pore volumes injected, fraction

q_o = oil production rate, STB/d

RMI = relative moles injected, fraction

R_s = solution GOR, scf/STB

R_p = producing GOR, scf/STB

RF = recovery factor, %

T_{mf} = matrix-fracture transfer term, ft

T_{res} = reservoir temperature, F

x_i = separator oil composition, mol%

y_i = separator gas composition, mol%

z_i = wellstream composition, mol%

Δp = pressure cycling interval, psia

Acknowledgments

The authors want to thank the management at EP Energy for permission to publish this paper. We would also like to thank Innovation Norway for providing funding to develop this technology.

References

Acuña, J. A. 2018. Straightforward Representative Fluid Flow Models for Complex Fracture Networks in Unconventional Reservoirs. Presented at SPE/AAPG/SEG Unconventional Resources Technology Conference, Houston, Texas, USA, 23-25 July. URTEC-2876208-MS. https://doi.org/10.15530/URTEC-2018-2876208.

Atan, S., Ajayi, A, Honarpour, M., Turek, E., Dillenbeck, E., Mock, C., Ahmadi and M., Pereira, C. 2018. The Viability of Gas Injection EOR in Eagle Ford Shale Reservoirs. Presented at the SPE Annual Technical Conference and Exhibition, Dallas, Texas, USA, 24-26 September. SPE-191673-MS. https://doi.org/10.2118/191673-MS.

Cheng, N. 2005. Special Topics on Developed Miscibility. PhD Dissertation presented to the Department of Petroleum Engineering and Applied Geophysics Norwegian University of Science and Technology, Trondheim, October.

Coats, K. H. 1989. Implicit Compositional Simulation of Single-Porosity and Dual-Porosity Reservoirs, Presented at the SPE Symposium on Reservoir Simulation in Houston, TX, February 6-8, 1989. SPE-18427-MS. https://doi.org/10.2118/18427-MS

Coats, K. H., Whitson, C. H. and Thomas, K. 2004. Modeling Conformance as Dispersion. Presented at the SPE Annual Technical Conference and Exhibition, 26-29 September, Houston, Texas. SPE-90390-PA. https://doi.org/10.2118/90390-PA

Fiallos, M., Yu, W., Ganjdanesh, R., Kerr, E., Sepehrnoori, K., Miao, J., and Ambrose, R., 2019. Modeling Interwell Fracture Interference and Huff-N-Puff Pressure Containment in Eagle Ford using EDFM. Presented at the SPE Oklahoma City Oil and Gas Symposium. SPE-195240-MS. https://doi.org/10.2118/195240-MS

Hamdi, H., Clarkson, C. R., Ghanizadeh, A., Ghaderi, S. M., Vahedian, A., Riazi, N. and A. Esmail. 2018. Huff-N-Puff Gas Injection Performance in Shale Reservoirs: A Case Study From Duvernay Shale in Alberta, Canada. Presented at SPE/AAPG/SEG Unconventional Resources Technology Conference, 23-25 July, Houston, Texas. URTEC-2902835-MS. https://doi.org/10.15530/URTEC-2018-2902835.

Hawthorne, S. B., Miller, J. D., Grabanski, C. B., Sorensen, J. A., Pekot, L. J., Kurz, B. A., Gorecki, C. D., Steadman, E.N. and Harju, J. A. 2017. Measured Crude Oil MMPs with Pure and Mixed CO_2, Methane, and Ethane and Their Relevance to Enhanced Oil Recovery from Middle Bakken and Bakken Shales. Presented at SPE Unconventional Resources Conference in Calgary, Alberta, Canada, 15-16 February. SPE-185072-MS. https://doi.org/10.2118/185072-MS.

Hearn, C.L. and Whitson, C.H. 1995. Evaluating Miscible and Immiscible Gas Injection in Safah Field, Oman. Presented at the 13th SPE Symposium on Reservoir Simulation, San Antonio, Feb. 12-15. SPE 29115. https://doi.org/10.2118/29115-MS

Hoda, M. F. and Whitson, C.H. 2013. Well Test Rate Conversion to Compositional Wellstream. Presented at the SPE Middle East Oil and Gas Show and Conference held in Manama, Bahrain, 10-13 March. SPE-164334-MS. https://doi.org/10.2118/164334-MS.

Hoffman, T. B. 2018. Huff-N-Puff Gas Injection Pilot Projects in the Eagle Ford. Presented at the SPE Canada Unconventional Resources Conference, 13-14 March, Calgary, Alberta, Canada. SPE-189816-MS. https://doi.org/10.2118/189816-MS.

Hoffman, T. B. 2019. Mechanisms for Huff-n-Puff Cyclic Gas Injection into Unconventional Reservoirs. Presented at the SPE Oklahoma City Oil and Gas Symposium, 9-10 April 2019, Oklahoma City, Oklahoma, USA. SPE-195223-MS. https://doi.org/10.2118/195223-MS.

Høier, L. and Whitson, C.H. 2000. Miscibility Variation in Compositionally Grading Reservoirs. Presented at the SPE Annual Technical Conference and Exhibition held in Dallas, Texas, 1-4 October. SPE-63086. https://doi.org/10.2118/49269-MS

Jessen, K. and Orr, F.M.Jr. 2008. On Interfacial-Tension Measurements to Estimate Minimum Miscibility Pressures, JPT (March). https://doi.org/10.2118/110725-PA

Jin, L., Hawthorne, S. B., Sorensen, J. et. al 2017. Utilization of Produced Gas for Improved Oil Recovery and Reduced Emissions from the Bakken Formation. Presented at the SPE Health, Safety, Security, Environment, & Social Responsibility Conference - North America, 18-20 April, New Orleans, Louisiana, USA. SPE-184414-MS. https://doi.org/10.2118/184414-MS.

Johns, R.T., Fayers, J.F., and Orr, F.M., Jr. 1992. Effect of Gas Enrichment and Dispersion on Nearly Miscible Displacement in Condensing/Vaporizing Drives. Presented at the Annual Technical Conference and Exhibition, Wash. D.C., Oct. 4-7. SPE-24938-PA. https://doi.org/10.2118/24938-PA.

Johns, R.T., Orr, F.M., Jr., and Dindoruk, B. 1992. Analytical Theory of Combined Condensing/Vaporizing Gas Drives. Presented at the SPE/DOE Symposium on Enhance Oil Recovery, Tulsa (April). SPE-24112-PA. https://doi.org/10.2118/24112-PA.

Kanfar, M.S. and Clarkson, C.R. 2017. Factors Affecting Huff-n-Puff Efficiency in Hydraulically-Fractured Tight Reservoirs. Presented at the SPE Unconventional Resources Conference, 15-16 February. SPE-185062-MS. https://doi.org/10.2118/185062-MS.

Lantz, R.B. 1971. Quantitative evaluation of numerical diffusion truncation error. Society of Petroleum Engineers Journal. SPE-2811-PA. https://doi.org/10.2118/2811-PA.

Lei, G., Cheng, N. and Whitson, C.H. 2014. Liquid-Rich Shale Versus Conventional Depletion Performance. Presented at the SPE/EAGE European Unconventional Resources Conference and Exhibition, Vienna, Austria, 25-27 February. SPE-167788-MS. https://doi.org/10.2118/167788-MS.

Liu, S., Sahni, V., Tan, J., Beckett, D. and Vo, T. 2018. Laboratory Investigation of EOR Techniques for Organic Rich Shales in the Permian Basin. Presented at SPE/AAPG/SEG Unconventional Resources Technology Conference, 23-25 July, Houston, Texas. URTEC-2890074-MS. https://doi.org/10.15530/URTEC-2018-2890074.

Orr, F.M., Jr., Johns, R.T., and Dindoruk, B. 1991. Miscibility in Four-Component Vaporizing Gas Drives. Presented at the SPE Annual Technical Conference and Exhibition (Oct. 6-9). SPE 22637. https://doi.org/10.2118/22637-PA.

Raterman, K.T., Farrell, H.E., Mora, O.S., Janssen, A.L., Gomez, G.A., Busetti, S., McEwen, J., Davidson, M., Friehauf, K., Rutherford, J., Reid, R., Jin, G., Roy, B. and Warren, M. 2017. Sampling a Stimulated Rock Volume: An Eagle Ford Example. Presented at SPE/AAPG/SEG Unconventional Resources Technology Conference, 24-26 July, Austin, Texas. URTeC-2670034. https://doi.org/10.15530/urtec-20172670034.

Sahni, V. and Liu, S. 2018. Miscible EOR Process Assessment for Unconventional Reservoirs: Understanding Key Mechanisms for Optimal Field Test Design. Presented at SPE/AAPG/SEG Unconventional Resources Technology Conference, 23-25 July, Houston, Texas. URTEC-2870010-MS. https://doi.org/10.15530/URTEC-2018-2870010.

Stalkup, F. I. Jr. 1984. Miscible Displacement, Monograph Series, Society of Petroleum Engineers.

Stalkup, F. I. Jr. 1990. Effect of Gas Enrichment and Numerical Dispersion on Enriched-Gas-Drive Predictions. Society of Petroleum Engineers Journal. SPE-18060-PA. https://doi.org/10.2118/18060-PA.

Tovar, F.D., Barrufet, M. A. and Schechter, D.S. 2018. Gas Injection for EOR in Organic Rich Shales. Part II: Mechanisms of Recovery. Presented at SPE/AAPG/SEG Unconventional Resources Technology Conference, 23-25 July, Houston, Texas. URTEC-2903026-MS. https://doi.org/10.15530/URTEC-2018-2903026.

Whitson, C.H. and Brulé, M. R. 2000. Phase Behavior, Monograph Series, Society of Petroleum Engineers.

Whitson, C.H. and Sunjerga, S. 2012. PVT in Liquid-Rich Shale Reservoirs. Presented at the SPE Annual Technical Conference and Exhibition, San Antonio, Texas, 8-10 October. SPE-155499-MS. https://doi.org/10.2118/155499-MS.

Whitson, C.H. and Torp, S.B. 1983. Evaluating Constant Volume Depletion Data, JPT (March), 610 620. https://doi.org/10.2118/10067-PA.

Zick, A.A. 1986. A Combined Condensing/Vaporizing Mechanism in the Displacement of Oil by Enriched Gases. Presented at the SPE Annual Technical Conference and Exhibition, New Orleans, Louisiana, 5-8 October. SPE-15493-MS. https://doi.org/10.2118/15493-MS.

Tables

Component	Composition mol%
H2S	0.00
N2	0.15
CO2	0.64
C1	63.09
C2	17.91
C3	10.83
I-C4	0.38
N-C4	0.80
I-C5	0.23
N-C5	0.33
C6	0.43
C7	0.52
C8	0.52
C9	0.42
C10	0.36
C11	0.31
C12	0.28
C13	0.25
C14	0.22
C15	0.20
C16	0.18
C17	0.16
C18	0.15
C19	0.13
C20	0.12
C21	0.11
C22	0.10
C23	0.09
C24	0.08
C25	0.08
C26p	0.94
Properties	
p_{sat}, psia	2500
GOR, scf/STB	1609
OGR, STB/MMscf	622
γ_{API}	44.3

** Based on a 2-stage separator process with $T_{sep,1}$ = 100 F, $p_{sep,1}$ = 150 psia and $T_{sep,2}$ = 60 F and $P_{sep,2}$ = 14.7 psia (standard conditions)*

Table 1a. The reservoir oil compositions used in the examples shown in this paper. This composition is synthetic (made up) and is just used for example purposes.

Component	Res. Oil mol%	Rich Gas mol%	Lean Gas mol%
H2S	0.00	0.00	0.0
N2	0.15	0.15	0.2
CO2	0.64	0.62	0.6
C1	63.09	66.79	91.8
C2	17.91	19.56	4.6
C3	10.83	11.77	1.8
I-C4	0.38	0.26	0.3
N-C4	0.80	0.49	0.5
I-C5	0.23	0.10	0.1
N-C5	0.33	0.12	0.1
C6	0.43	0.08	0.1
C7+	5.21	0.06	0.0
Total	**100**	**100**	**100**

Table 1b. Comparison of the reservoir oil composition (details showed in Table 1) and the *rich* and *lean* injection gas referenced in this paper. These compositions are synthetic (made up) and is just used for example purposes.

Component	Mol Wt	Tc (R)	Pc (psia)	Crit Z	Vol Tran	AF	A	B	Tb (R)	Visc Zc	LMW
H2S	34.1	672.1	1300.0	0.29	0.1015	0.0900	0.42748	0.08664	382.4	0.283	
N2	28.0	227.2	492.8	0.29	-0.0009	0.0370	0.42748	0.08664	139.4	0.292	
CO2	44.0	547.4	1069.5	0.29	0.2175	0.2250	0.42748	0.08664	333.3	0.274	
C1	16.0	343.0	667.0	0.29	-0.0025	0.0110	0.42748	0.08664	201.6	0.286	
C2	30.1	549.6	706.6	0.29	0.0589	0.0990	0.42748	0.08664	332.7	0.279	
C3	44.1	665.7	616.1	0.29	0.0908	0.1520	0.42748	0.08664	416.2	0.276	
I-C4	58.1	734.1	527.9	0.29	0.1095	0.1860	0.42748	0.08664	471.1	0.282	
N-C4	58.1	765.2	550.6	0.29	0.1103	0.2000	0.42748	0.08664	491.1	0.274	
I-C5	72.2	828.7	490.4	0.29	0.0977	0.2290	0.42748	0.08664	542.4	0.272	
N-C5	72.2	845.5	488.8	0.29	0.1195	0.2520	0.42748	0.08664	557.0	0.268	
C6	83.6	921.8	475.0	0.29	0.1343	0.2507	0.42748	0.08664	608.7	0.269	76.9
C7	96.7	983.9	439.7	0.29	0.1452	0.2859	0.42748	0.08664	660.5	0.264	90.1
C8	110.4	1038.7	404.8	0.29	0.1568	0.3256	0.42748	0.08664	709.5	0.260	103.9
C9	123.8	1087.9	372.5	0.29	0.1744	0.3675	0.42748	0.08664	755.8	0.256	117.5
C10	137.1	1131.7	344.6	0.29	0.1913	0.4088	0.42748	0.08664	798.5	0.252	130.8
C11	150.3	1171.4	320.3	0.29	0.2074	0.4496	0.42748	0.08664	838.5	0.248	144.0
C12	163.4	1207.6	299.0	0.29	0.2227	0.4898	0.42748	0.08664	875.9	0.245	157.2
C13	176.5	1240.9	280.3	0.29	0.2370	0.5293	0.42748	0.08664	911.0	0.242	170.3
C14	189.4	1271.6	263.8	0.29	0.2505	0.5681	0.42748	0.08664	944.1	0.239	183.3
C15	202.3	1300.0	249.1	0.29	0.2630	0.6062	0.42748	0.08664	975.3	0.236	196.2
C16	215.1	1326.5	236.0	0.29	0.2746	0.6436	0.42748	0.08664	1004.7	0.233	209.0
C17	227.7	1351.2	224.3	0.29	0.2854	0.6803	0.42748	0.08664	1032.6	0.230	221.7
C18	240.3	1374.4	213.8	0.29	0.2953	0.7163	0.42748	0.08664	1059.1	0.227	234.3
C19	252.8	1396.2	204.3	0.29	0.3045	0.7516	0.42748	0.08664	1084.2	0.224	246.8
C20	265.1	1416.7	195.7	0.29	0.3129	0.7863	0.42748	0.08664	1108.1	0.222	259.2
C21	277.4	1436.1	187.9	0.29	0.3206	0.8203	0.42748	0.08664	1130.9	0.219	271.5
C22	289.6	1454.4	180.8	0.29	0.3277	0.8536	0.42748	0.08664	1152.6	0.216	283.7
C23	301.6	1471.9	174.3	0.29	0.3342	0.8863	0.42748	0.08664	1173.3	0.214	295.8
C24	313.5	1488.5	168.4	0.29	0.3402	0.9183	0.42748	0.08664	1193.1	0.212	307.8
C25	325.4	1504.3	163.0	0.29	0.3457	0.9498	0.42748	0.08664	1212.1	0.209	319.7
C26p	381.5	1571.8	141.9	0.29	0.3663	1.0943	0.42748	0.08664	1293.9	0.199	331.5

Table 2a. Component properties of the "generic" Soave-Redlich-Kwong (SRK) equation of state (EOS) model used for example simulations in this paper.

Comp	H2S	N2	CO2	C1
H2S	0			
N2	0	0		
CO2	0	0	0	
C1	0.08	0.02	0.12	0
C2	0.07	0.06	0.12	0
C3	0.07	0.08	0.12	0
I-C4	0.06	0.08	0.12	0
N-C4	0.06	0.08	0.12	0
I-C5	0.06	0.08	0.12	0
N-C5	0.06	0.08	0.12	0
C6	0.05	0.08	0.12	0
C7	0.03	0.08	0.1	0.0149
C8	0.03	0.08	0.1	0.0173
C9	0.03	0.08	0.1	0.0197
C10	0.03	0.08	0.1	0.0219
C11	0.03	0.08	0.1	0.024
C12	0.03	0.08	0.1	0.026
C13	0.03	0.08	0.1	0.0278
C14	0.03	0.08	0.1	0.0295
C15	0.03	0.08	0.1	0.0311
C16	0.03	0.08	0.1	0.0325
C17	0.03	0.08	0.1	0.0339
C18	0.03	0.08	0.1	0.0352
C19	0.03	0.08	0.1	0.0364
C20	0.03	0.08	0.1	0.0374
C21	0.03	0.08	0.1	0.0385
C22	0.03	0.08	0.1	0.0394
C23	0.03	0.08	0.1	0.0403
C24	0.03	0.08	0.1	0.0411
C25	0.03	0.08	0.1	0.0419
C26p	0.03	0.08	0.1	0.045

Table 2b: BIPS of the "generic" SRK EOS model used for example simulations in this paper. Values not presented in this table is 0.

Figures

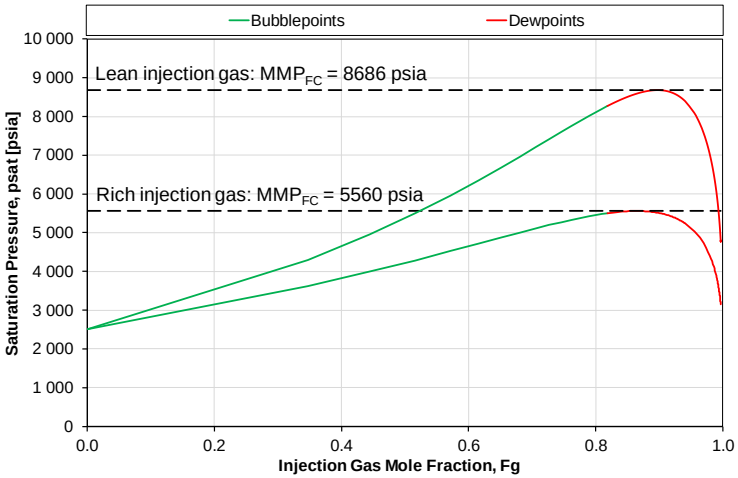

Fig. 1. Swell test for reservoir oil with *lean* (MMP$_{FC}$ = 8686 psia) and *rich* injection gas (MMP$_{FC}$ = 5560 psia) Temperature = 250 F.

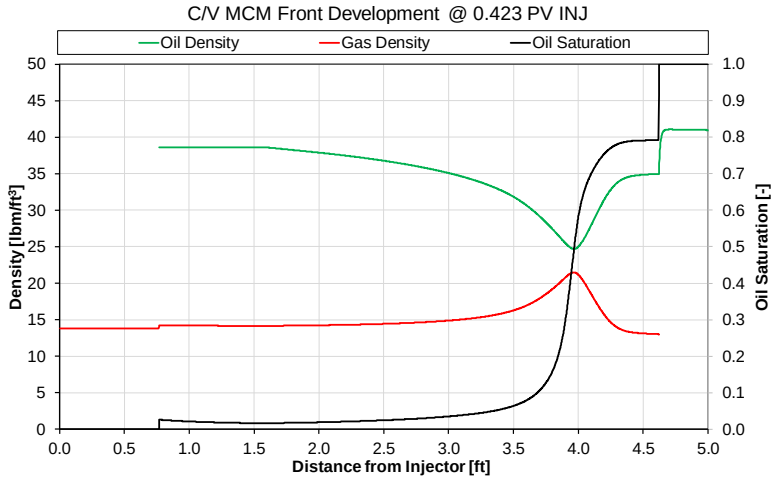

Fig. 2. C/V front at 0.423 pore volumes injected for an undersaturated oil w/ bubblepoint 2500 psia. Injection pressure is 4500 psia. MMP$_{C/V}$ is 4157 psia, MMP$_{FC}$ is 5560 psia.

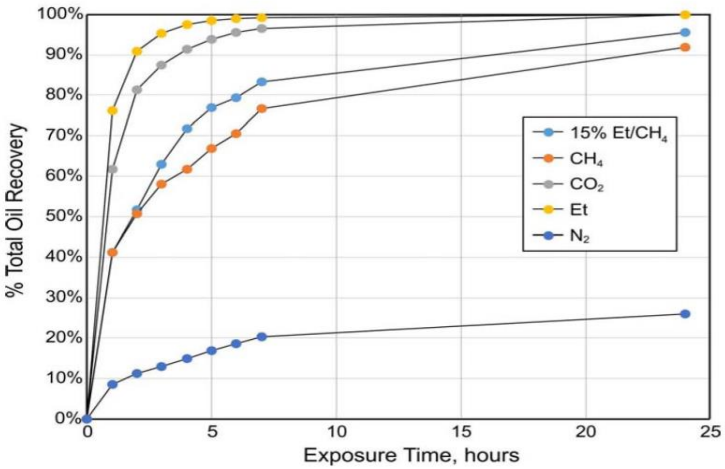

Fig. 3. Oil recovery from Middle Bakken core plug with different injectants (Hawthorne et. al, 2017). N_2 and CH_4 were at p = 6000 psia, all other fluids were at 5000 psia. T = 230 F.

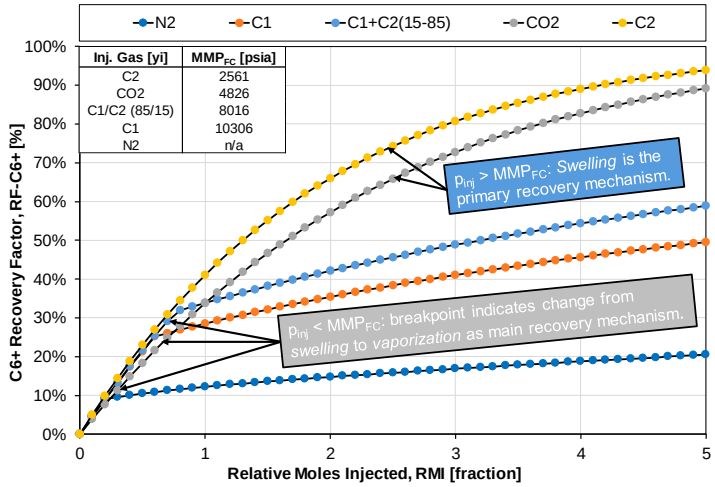

Fig. 4. Simulated *constant volume injection* (CVI) experiment at p = 5000 psia and T = 250 F mimicking the results by Hawthorne et al. (2017). Reservoir oil given in Table 1.

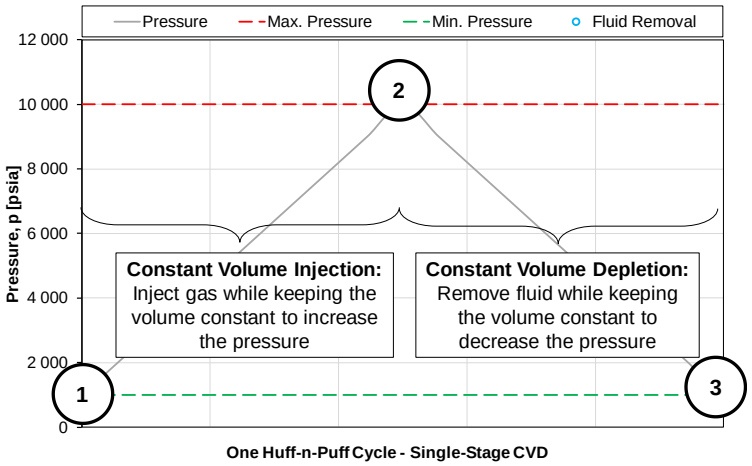

Fig. 5. Conceptual illustration of pressure cycling in a HnP PVT Experiment with a *single-stage CVD experiment* during the production (puff) part of the HnP cycle.

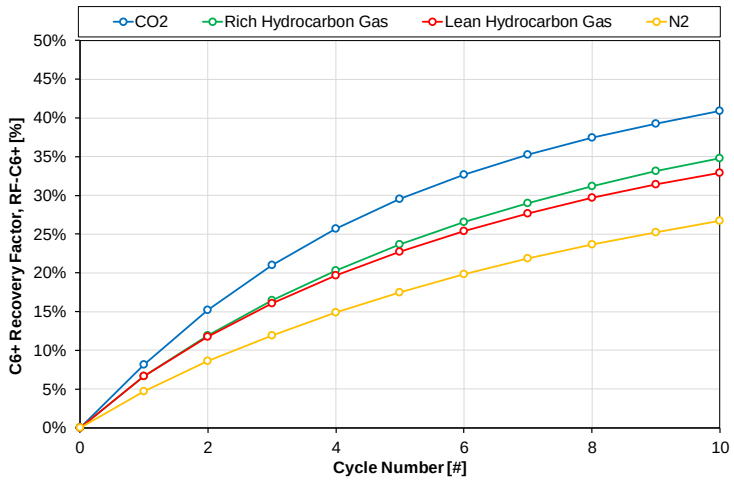

Fig. 6. Recovery of C_{6+} components in a simulated HnP PVT experiment with pressure cycling from 1000 psia to 6000 psia (Δp = 5000 psia).

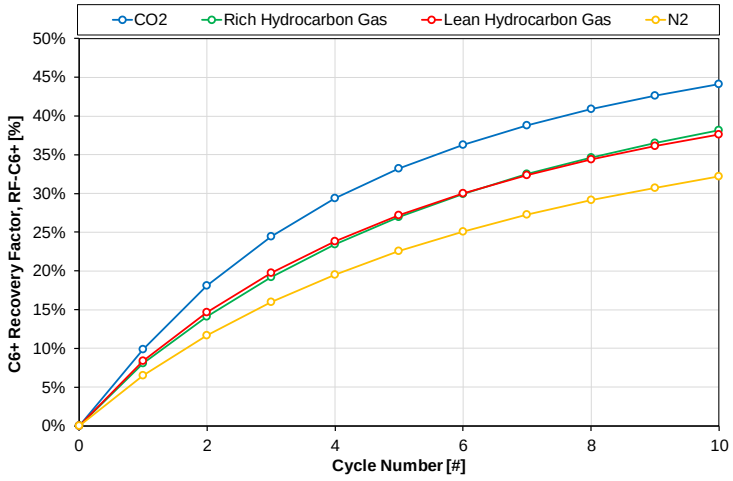

Fig. 7. Recovery of C_{6+} components in a simulated HnP PVT experiment with pressure cycling from 1000 psia to 10000 psia (Δp = 9000 psia).

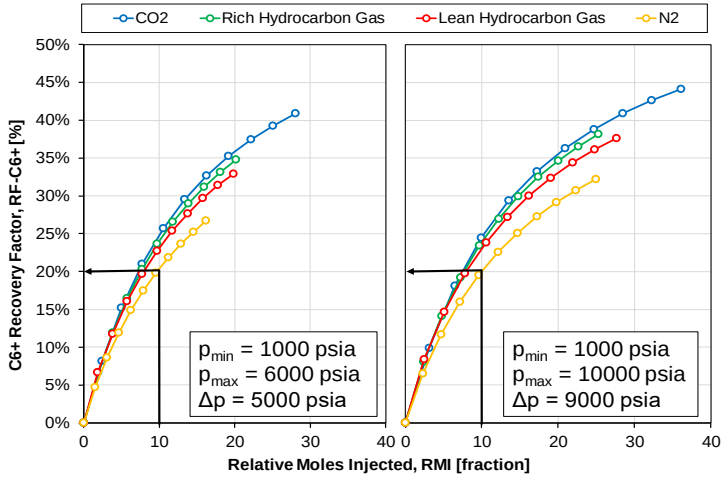

Fig. 8. Recovery of C_{6+} versus relative moles injected ("recovery efficiency plot") for pressure cycling interval between 1000-6000 psia (left) and 1000-10000 psia (right). The recovery is the same in the two cases, i.e. the same RMI injected, yield the same recovery.

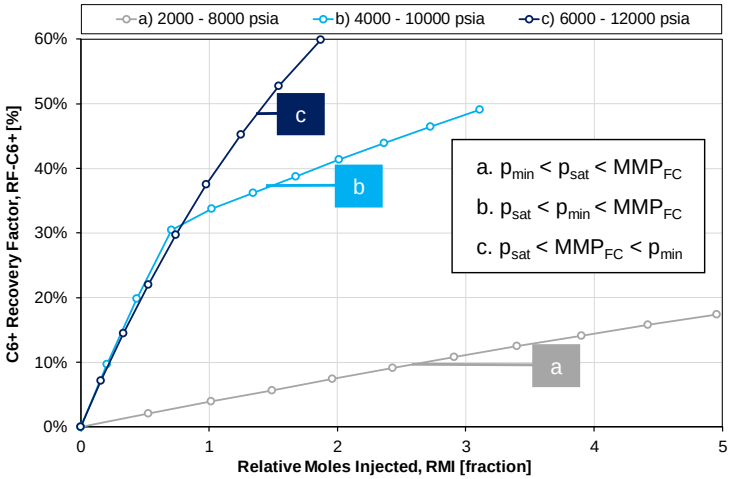

Fig. 9. Recovery vs. relative moles injected for different p_{min}, relative to the first contact miscibility pressure & saturation pressure, but for the same pressure cycling Δp = 6000 psia.

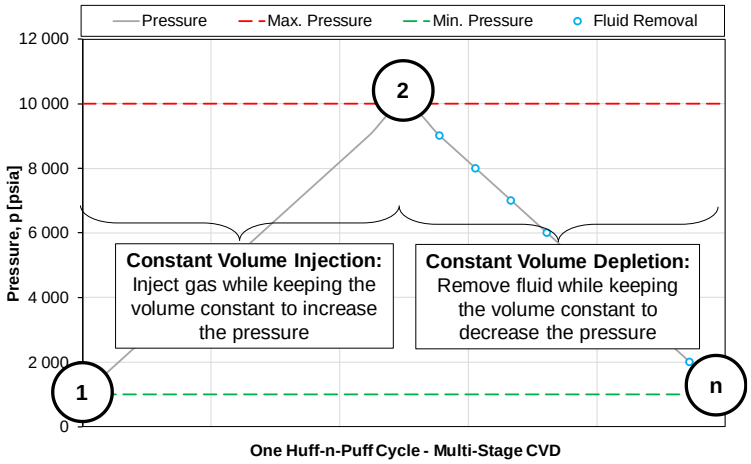

Fig. 10. Conceptual illustration of pressure cycling in a HnP PVT Experiment with a *multi-stage CVD experiment* during the production (puff) part of the HnP cycle.

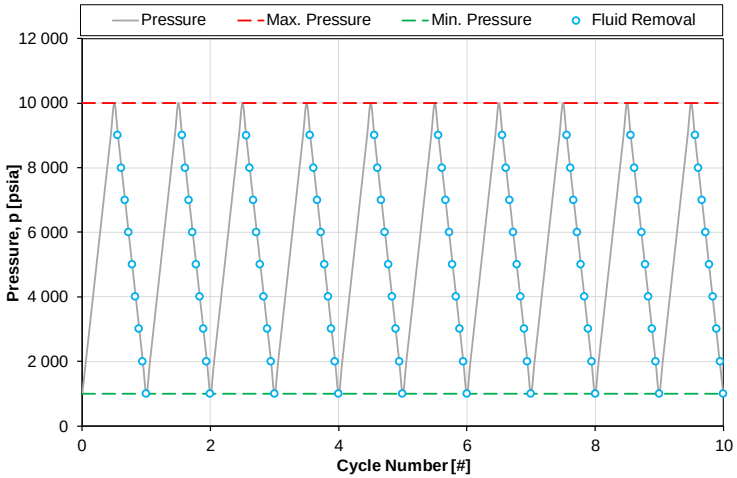

Fig. 11. Conceptual illustration of the HnP PVT experiment with Multi-Stage CVD with 10 pressure cycles from 1000 psia to 10000 psia (Δp = 9000 psia).

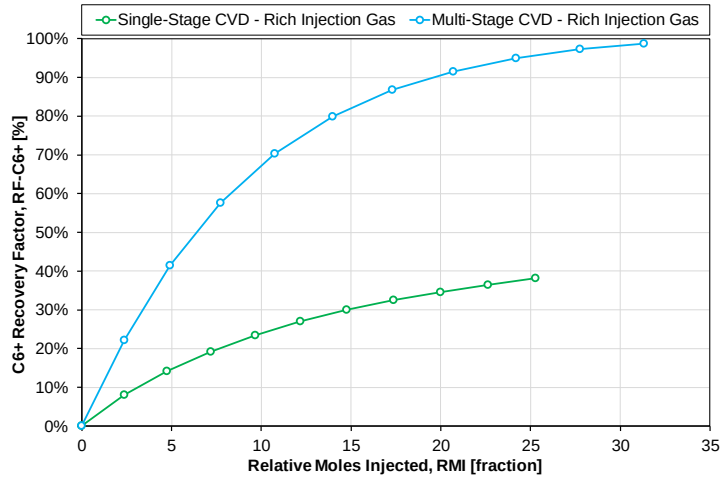

Fig. 12. Performance difference between the HnP PVT experiment with Single-Stage CVD versus Multi-Stage CVD during the "production/depletion" (puff) part of each cycle with 10 pressure cycles from 1000 psia to 10000 psia (Δp = 9000 psia).

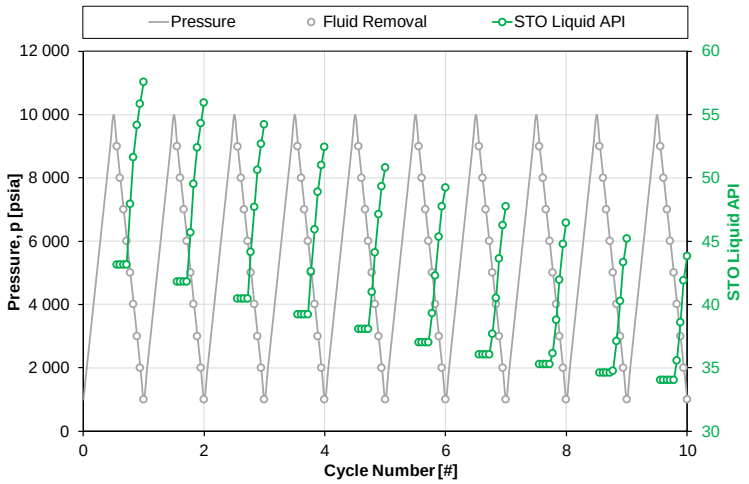

Fig. 13a. Stock tank liquid API for the compositions removed from the PVT cell ("produced") at different stages and cycles.

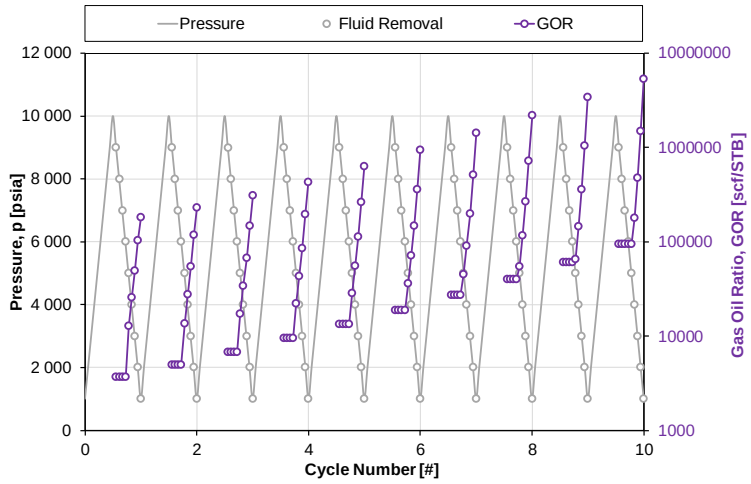

Fig. 13b. Solution GOR (R_s) for the compositions removed from the PVT cell ("produced") at different stages and cycles.

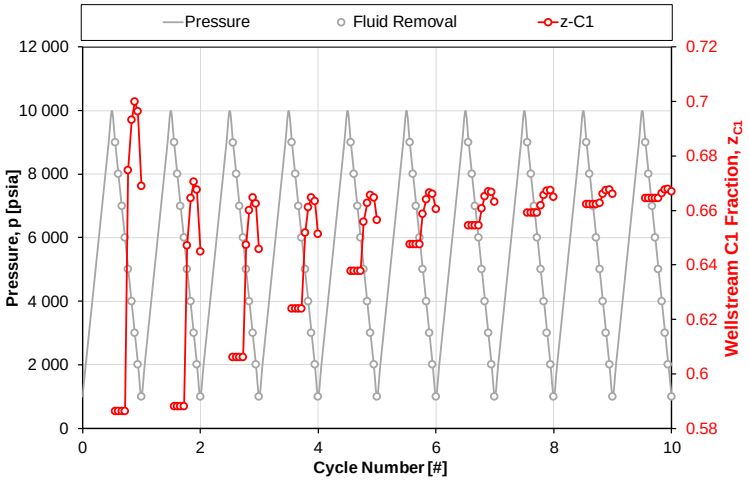

Fig. 13c. Wellstream C_1 for the compositions removed from the PVT cell ("produced") at different stages and cycles.

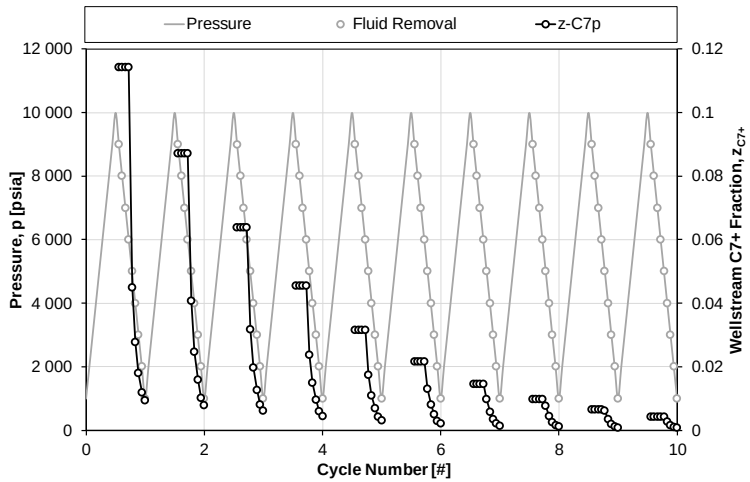

Fig. 13d. Wellstream C_{7+} for the compositions removed from the PVT cell ("produced") at different stages and cycles.

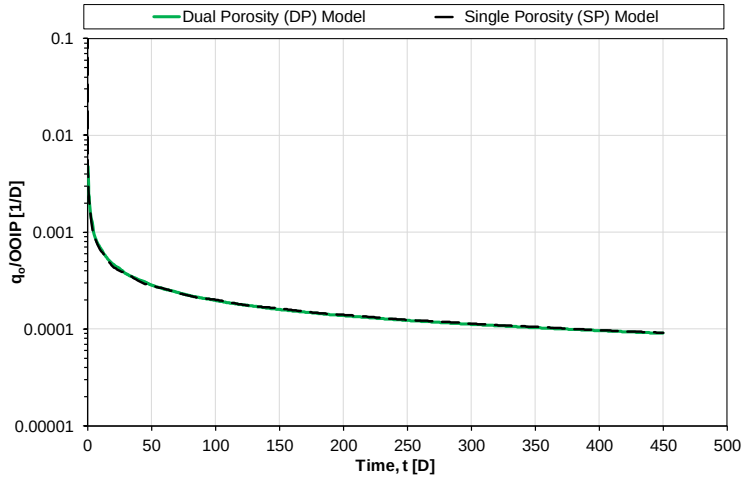

Fig. 14a. Dual porosity (DP) model that mimics the single porosity (SP) model performance – *q_o/OOIP* versus time for primary depletion.

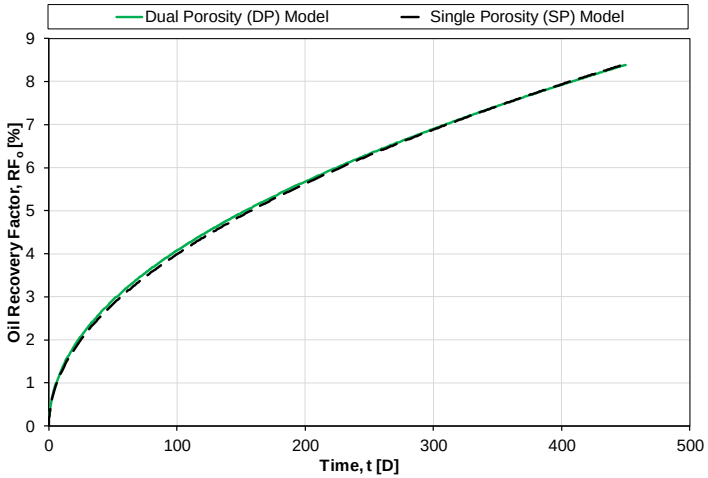

Fig. 14b. Dual porosity (DP) model that mimics the single porosity (SP) model performance – *oil recovery* versus time for primary depletion.

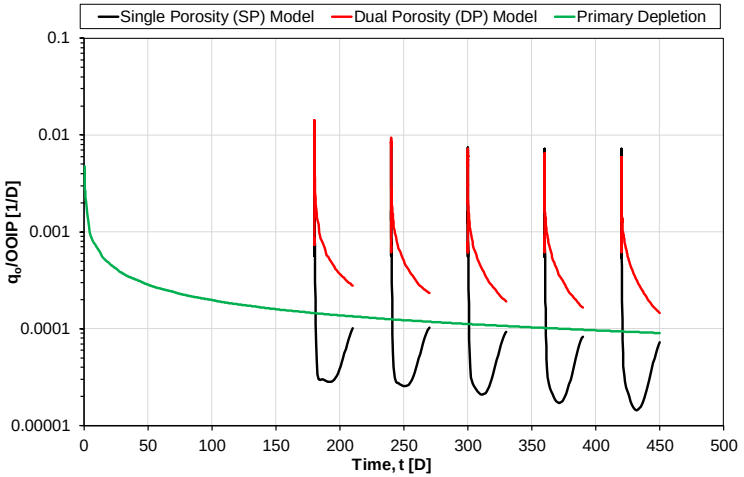

Fig. 15a. Gas HnP performance (*q_o/OOIP)* comparison of a dual porosity (DP) simulation model and a single porosity (SP) simulation model. Note how the SP model yields no additional recovery, while the DP model yields significant uplift.

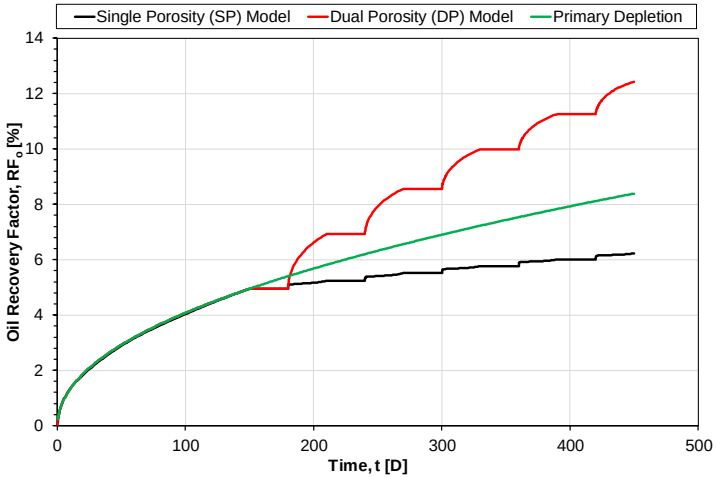

Fig. 15b. Gas HnP performance (*oil recovery*) comparison of a dual porosity (DP) simulation model and a single porosity (SP) simulation model. Note how the SP model yields no additional recovery, while the DP model yields significant uplift.

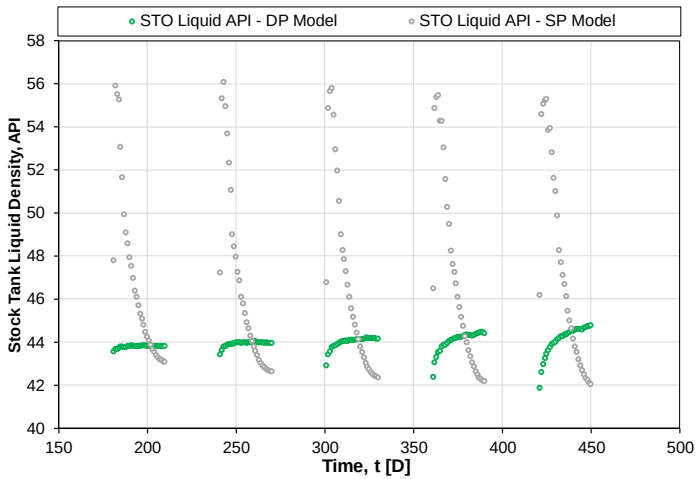

Fig. 16a. Stock tank liquid API versus time for a single-porosity (SP) model (*no incremental uplift*) and a dual-porosity (DP) model (*significant uplift*).

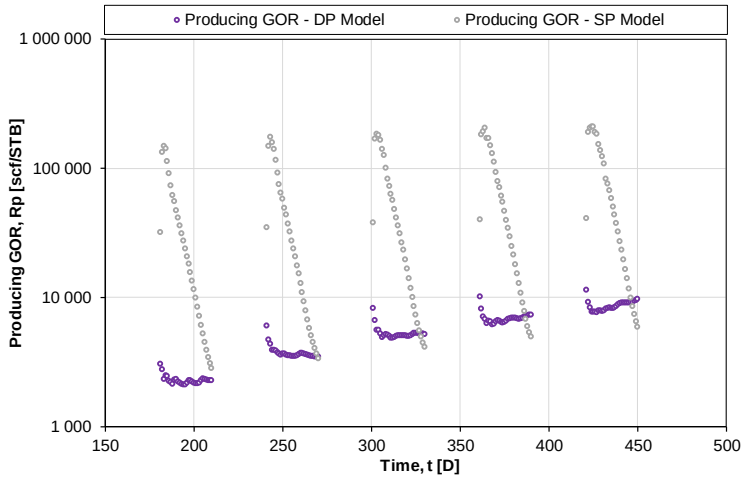

Fig. 16b. Producing GOR (R_p) versus time for a single-porosity (SP) model (*no incremental uplift*) and a dual-porosity (DP) model (*significant uplift*).

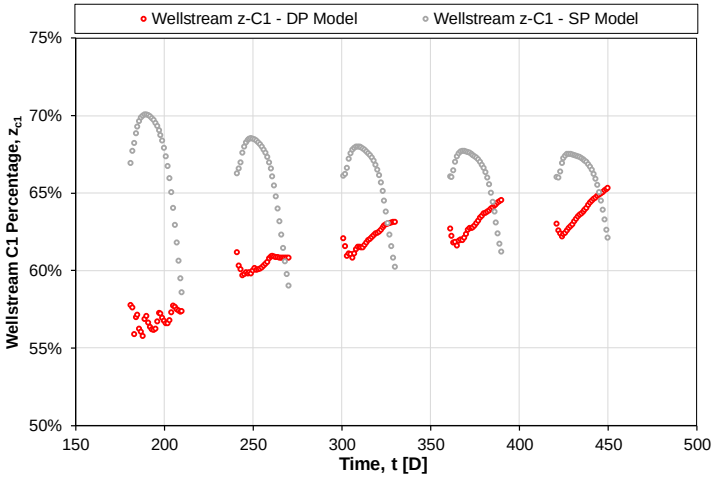

Fig. 16c. Wellstream C_1 versus time for a single-porosity (SP) model (*no incremental uplift*) and a dual-porosity (DP) model (*significant uplift*).

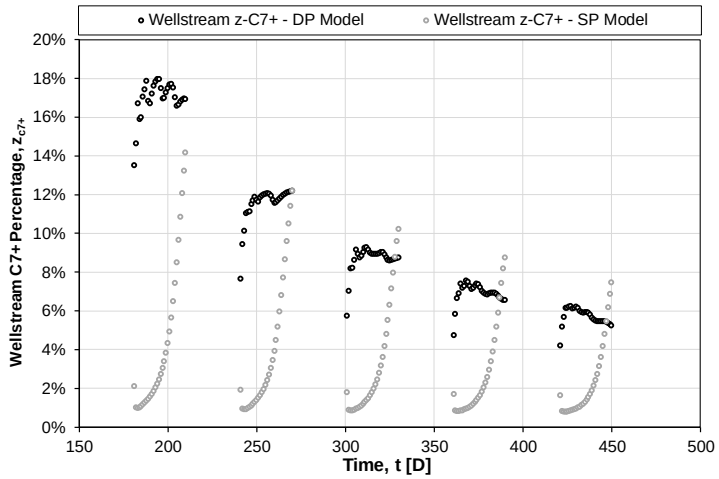

Fig. 16d. Wellstream C_{7+} versus time for a single-porosity (SP) model (*no incremental uplift*) and a dual-porosity (DP) model (*significant uplift*).

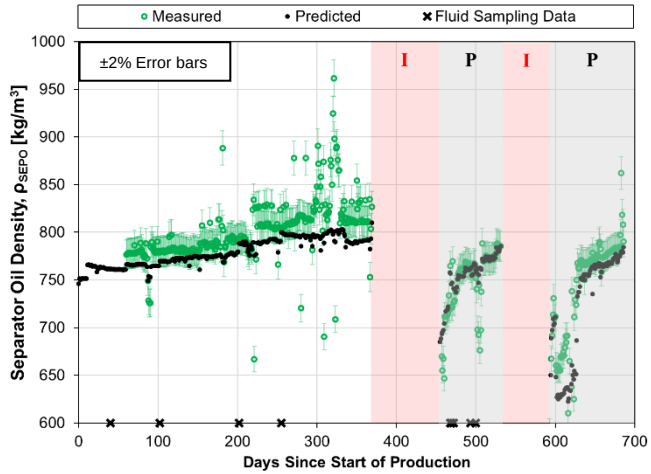

Fig. 17. Separator oil density, predicted vs. measured, HnP *injection* well

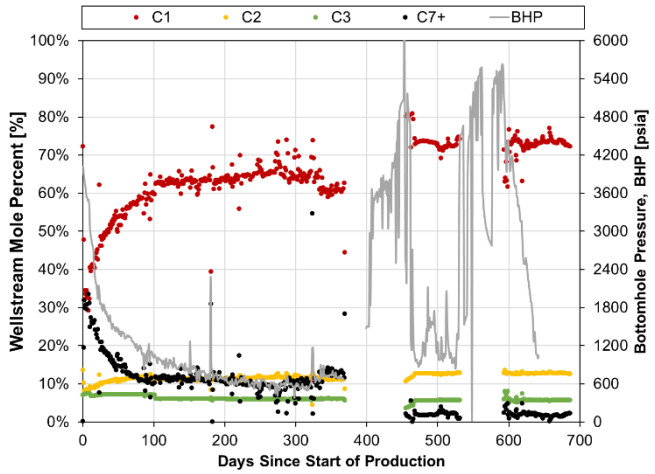

Fig. 18. Calculated wellstream composition | BHP vs time - HnP *injection* well

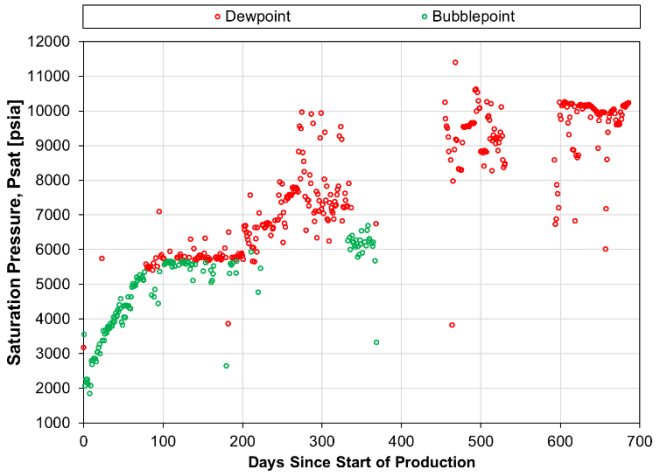

Fig. 19. Calculated wellstream saturation pressure vs time, HnP *injection* well

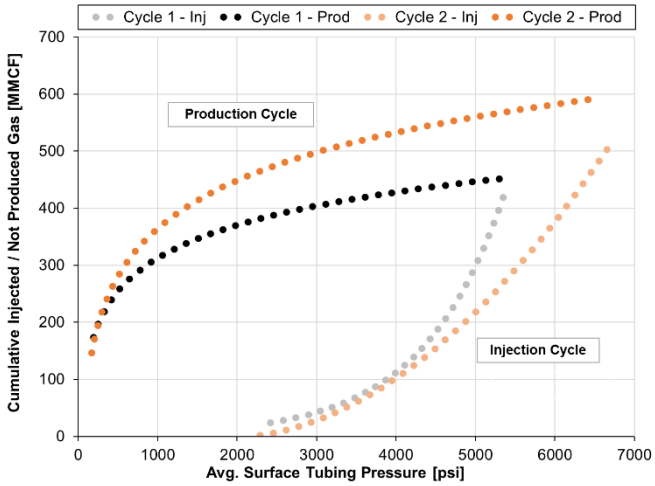

Fig. 20. Example of a “Hammock” pressure build-up (injection/huff) and decline (production/puff) curve. Significant *hysteresis* observed.

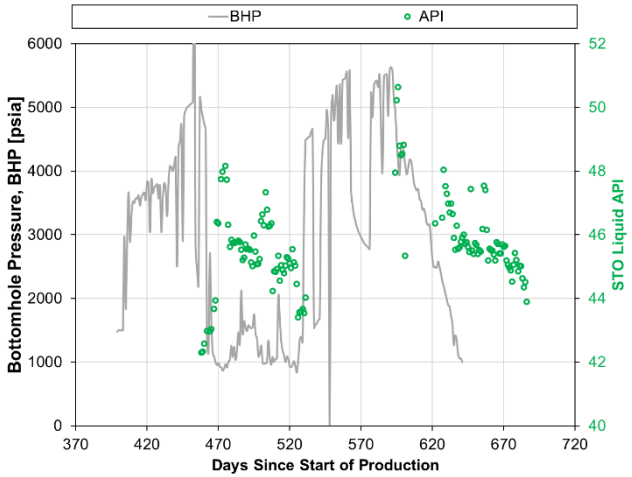

Fig. 21a. Calculated API and BHP vs. time, HnP *injection* well

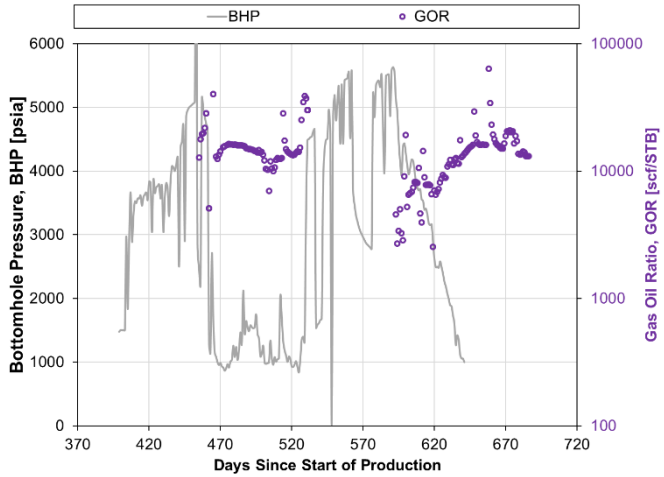

Fig. 21b. Calculated GOR and BHP vs. time, HnP *injection* well

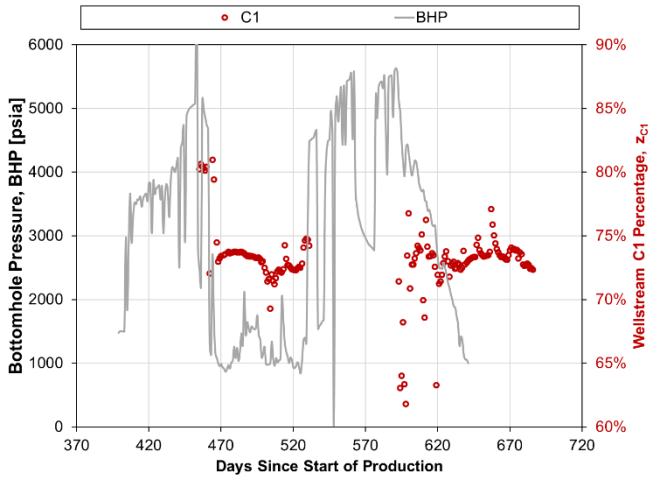

Fig. 21c. Calculated wellstream C_1 and BHP vs. time, HnP *injection* well

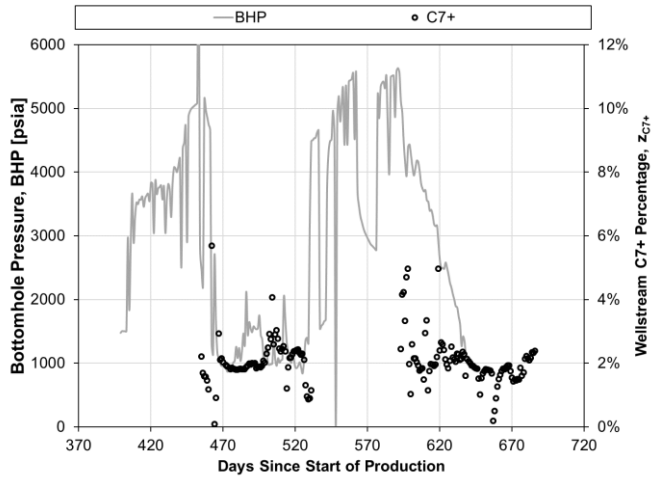

Fig. 21d. Calculated wellstream C_{7+} and BHP vs. time, HnP *injection* well